Transactions of the Korean Nuclear Society Spring Meeting
Jeju, Korea, May 22-23, 2025

Optimized Temperature for Thermal Oxidation of Silver for Iodine Separation in Fission ^{99}Mo Production Process

Bogyeong Park, Jin-hee Kim*, Suseung Lee, and Seung-Kon Lee
Radioisotope Research Division, Korea Atomic Energy Research Institute, 111 Daedeok-daero 989beon-gil, Yuseong-gu, Daejeon, 34057 Republic of Korea
**Corresponding author:kimjinhee@kaeri.re.kr*

***Keywords : Fission ^{99}Mo, Iodine removal, Silver oxide, Thermal oxidation**

1. Introduction

Molybdenum-99 (^{99}Mo), the parent nuclide of Technetium-99m (^{99m}Tc), is the most widely used medical radioisotope worldwide. However, its supply is limited due to the aging of major production facilities, and various efforts have been made to secure a stable supply of ^{99}Mo. As part of these efforts, the Korea Atomic Energy Research Institute (KAERI) has been conducting research on fission-based ^{99}Mo production through a research reactor construction project since 2012. KAERI's fission-Mo production involves the dissolution of a plate-type low-enriched uranium (LEU) target using a highly concentrated sodium hydroxide solution. Various byproducts (uranium and transuranic compounds, radioactive iodine compounds, and radioactive gases) generated in this process must be removed before molybdenum separation to get the high purity of ^{99}Mo. This study aims to optimize the synthesis of a Silver-coated alumina precipitant for effective iodine separation from the LEU target dissolution solution in KAERI's fission-Mo production process and to determine the optimal synthesis conditions. [1]

1.1. Silver-Based Iodine Removal Mechanism

In the iodine removal reaction, silver ions (Ag^+) and iodide ions (I^-) exhibit high reactivity, leading to the rapid formation of silver iodide (AgI). Due to AgI's low solubility ($K_{sp} = 8.3\times10^{-17}$), it precipitates immediately upon formation, making it widely used for iodine removal in aqueous environments. [2] Silver oxides (Ag_2O, AgO, Ag_2O_2, etc.) dissolve in alkaline conditions, releasing $[Ag(OH)_2]^-$ complex ions that dissociate to release Ag^+, thereby promoting AgI formation. Compared to other silver compounds (AgCl, Ag_2SO_4, $AgNO_3$, $[Ag(NH_3)_2]^+$, etc.), silver oxide is relatively stable and dissolves slowly, allowing a continuous supply of silver ions during the iodine separation process.

1.2. Effect of Thermal treatment Temperature on Silver Oxide Formation

Several factors, including temperature, time, and pressure, influence silver oxide formation during thermal treatment. Among these, temperature has the most significant impact due to the Arrhenius law, which states that reaction rates and oxygen diffusion rates increase exponentially with temperature. [3]

Silver oxidation begins at 150°C, and at higher temperatures, the crystal lattice spacing increases, leading to crystal growth. Between 250-350°C, the silver oxide crystal structure collapses, and necking between crystals occurs. [4]

This study used the silver mirror reaction [5], which allows easy control of particle size, to coat silver onto alumina. Thermal treatment under an oxygen atmosphere was then applied to oxidize the silver. The effects of thermal treatment temperature on the amount and crystal size of silver oxide were analyzed to determine optimal conditions.

2. Experimental Methods

2.1. Materials

Spherical alumina (DENKA, DAW-70, average particle size 74.6 μm) was used as the support due to its resistance to alkalinity and radiation. The reagents used in this study included silver nitrate (ACS, 99.9+%, Alfa Aesar), ammonia solution (25%, Sigma-Aldrich), potassium hydroxide (pellets, 85.0%, SAMCHUN), D-(+)-glucose (ACS, Sigma-Aldrich), potassium iodide (ReagentPlus, 99%, Sigma-Aldrich), and sodium thiosulfate (ReagentPlus, 99%, Sigma-Aldrich). All solutions were prepared using ultrapure water (Avidity Science, Cascada, 18.2 MΩ·cm at 25°C).

2.2. Silver Coating and Oxidation

2.2.1. Silver Reduction

All reactions were conducted at room temperature (20°C) with stirring at 150 rpm using a shaker. A 250 mL polypropylene container was filled with 50 g of washed alumina, 86.24 mL of water, and Tollens' reagent (0.5 M $AgNO_3$ 12.5 mL, 25% NH_4OH 1.26 mL), followed by stirring for 30 minutes. Then, 6.875 mL of 0.5 M glucose was added and stirred for 10 minutes. Afterward, 13.7 mL of 0.8 M KOH was added and stirred for an additional 30 minutes. The sample was washed three times with ultrapure water and dried at 80°C for over 12 hours.

2.2.2. Silver Oxidation

The silver-coated alumina was placed in an alumina boat crucible and heat-treated under an oxygen atmosphere (0.01 MPa) in a tubular furnace at 150, 200, 250, and 300°C for 4 hours (heating/cooling rate: 5°C/min). Particles finer than 325 mesh (45 µm) were removed after processing.

3. Results and Discussion

3.1. Surface Morphology Analysis

The surface morphology of the synthesized silver-coated alumina was examined using a Field Emission Scanning Electron Microscope (FE-SEM, SU8220, Hitachi). Silver nanoparticles formed via the silver mirror reaction were observed to be spherical or irregular, as shown in Fig. 1. Silver and silver oxide particles, which appear silver-gray and dark brown, respectively, were identified. Over-reduced black silver particles observed before thermal treatment were fragmented into smaller particles after oxidation. At 150°C, silver nanoparticles were well distributed on the surface, while higher temperatures resulted in a darker brown color, indicating increased oxidation. At 300°C, broken or detached silver oxide particles were observed.

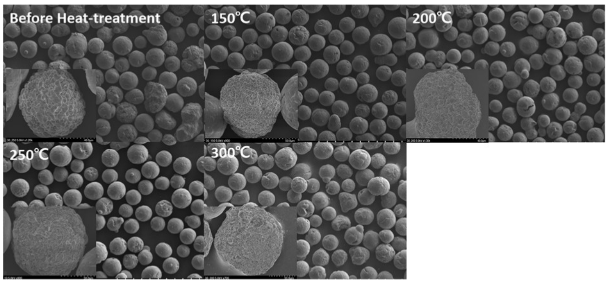

Fig. 1. Scanning Electron Microscope (SEM) Images of Silver-coated Alumina

3.2. Total Ag and Ag_2O Quantification

To determine the total silver and silver oxide content, 0.5 g of the sample was reacted with 5 mL of 3N HNO_3 (for total Ag) or 6N NaOH (for Ag_2O) in an ultrasonicator for 30 or 60 minutes. And the concentration of silver was measured using a Atomic Absorption Spectrometer (AA, GFA-7000A, Shimadzu).

The total silver content was highest at 200°C, while a lower amount was observed at higher temperatures, likely due to excessive particle agglomeration causing detachment and spalling. The silver oxide content remained constant at 0.011 mg/g for thermal treatments between 150°C and 250°C but decreased to 0.009 mg/g at 300°C due to spalling. The oxidation ratio was highest at 250°C, indicating that under the same reduction and thermal treatment conditions, the optimal temperature is 250°C.

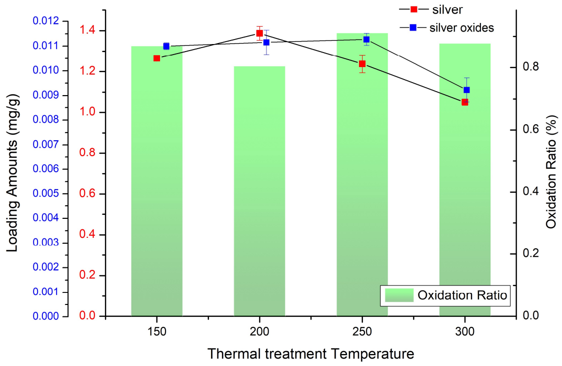

Fig. 2. Effect of Thermal Treatment Temperature on Silver Loading

3.3. Crystal Size Analysis

X-ray Diffraction (XRD, Panalytical, EMPYREAN) was used to analyze the crystal structure.

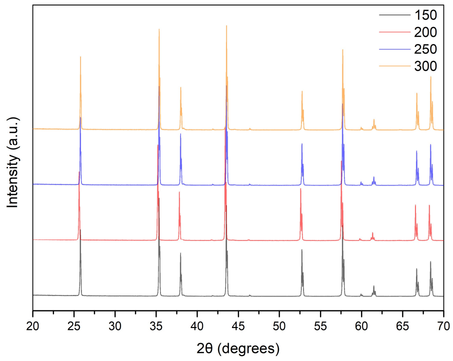

Fig. 3. X-ray diffraction (XRD) Spectra of Silver-coated alumina at Different Thermal treatment Temperature

On the spectra, the major peaks of silver (37.7˚, 43.3˚), silver oxides (57.5˚, 66.5˚, 68.2˚), and alumina (25.6˚, 35.1˚, 52.5˚) were observed.

The Scherrer equation (1) was applied to calculate the mean of Ag_2O crystal sizes, which ranged from 208-238 nm. Higher thermal treatment temperatures led to increased mean crystal size due to Ostwald ripening, as shown in Fig. 4.

$$(1)\ \ D = \frac{K\lambda}{\beta cos\theta}$$

where D represents the average crystallite size, and K is a constant related to crystallite shape (0.9), λ is the X-ray wavelength, β is the full width at half maximum of the diffraction peak in radians, and θ is the bragg diffraction angle.

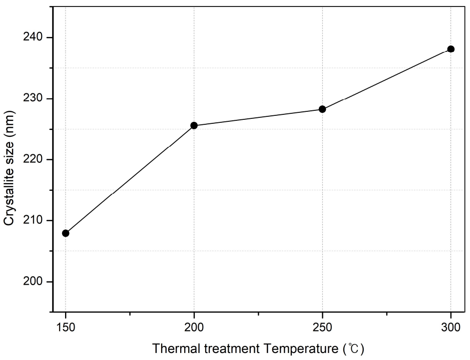

Fig. 4. Average Crystallite Size of Ag_2O of Silver-coated alumina at Different Thermal treatment Temperature

4. Conclusion

In this study, the amount and oxidation ratio of silver oxide and the size of the formed crystals at various thermal oxidation temperatures were investigated.

The experimental results showed that the silver oxide content remained stable at approximately 0.011 mg/g within the temperature range of 200–250°C. However, at 300°C, excessive particle agglomeration and detachment led to a decrease in silver oxide content to 0.009 mg/g. Additionally, the highest oxidation efficiency was observed at 250°C. The silver oxide crystals attached to the alumina surface had an average size of 208-238 nm, and their size increased as the thermal oxidation temperature increased.

The dissolution rate of silver oxide is influenced by various operating conditions such as flow rate, pH, and temperature. Therefore, it is necessary to further investigate its dissolution behavior based on the calculated silver oxide crystallite size under actual operating conditions. To ensure rapid iodine removal while continuously supplying silver ions until the end of operation, adjusting the particle size to suit the operating conditions is crucial for system performance. Optimizing these factors is expected to further enhance the efficiency and longevity of the iodine removal system.

REFERENCES

[1] Lee, S. K., Lee, S., Kang, M., Woo, K., Yang, S. W., & Lee, J. (2020). Development of fission 99Mo production process using HANARO. Nuclear Engineering and Technology, 52(7), 1517-1523.

[2] Riley, B. J., Vienna, J. D., Strachan, D. M., McCloy, J. S., & Jerden Jr, J. L. (2016). Materials and processes for the effective capture and immobilization of radioiodine: A review. Journal of Nuclear Materials, 470, 307-326.

[3] Nagy, A., & Mestl, G. (1999). High temperature partial oxidation reactions over silver catalysts. Applied Catalysis A: General, 188(1-2), 337-353.

[4] Mazlan, M. R., Jamadon, N. H., Rajabi, A., Sulong, A. B., Mohamed, I. F., Yusof, F., & Jamal, N. A. (2023). Necking mechanism under various sintering process parameters–A review. journal of materials research and technology, 23, 2189-2201.

[5] Qu, L., & Dai, L. (2005). Novel silver nanostructures from silver mirror reaction on reactive substrates. The Journal of Physical Chemistry B, 109(29), 13985-13990.